7/246

P. 31

NASA Lewis Research Center
Attn: Ms. Lorene Albergottie,
Grants Officer
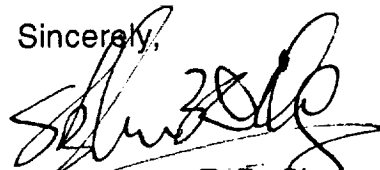Mail Stop 500-315
Cleveland, Ohio 44135

June 1, 1992

Subject: Final Technical Report, Grant NAG3-1288, "The Study of the
Thermal Behavior of a New Semicrystalline Polyimide"

Researchers: Dr. Stephen Z.D. Cheng
Ms. Tammy M. Chalmers

Employer: University of Akron
Department of Polymer Science
Akron, Ohio 44325-3909

The enclosed paper entitled "Thermal Properties of a Tough, New Semicrystalline Polyimide" details the research conducted under this grant. This paper which includes acknowledgement of this grant has been submitted to *Polymer International* for publication and is currently under review. As indicated on the enclosed New Technology Report Form, the research described here did not produce any patentable inventions or discoveries. Also, this grant was used in order to financially support a graduate student, so no equipment was purchased with these funds. If any further documentation or clarification is required in order to close out this grant, please notify Ms. Tammy Chalmers at (216) 972-7538. Three copies of this report are enclosed for your distribution. Two additional copies have been sent to the NASA Scientific and Technical Information Facility in Maryland. Thank you for your cooperation.

Sincerely,

Dr. Stephen Z. D. Cheng

NASA GRANTEE
NEW TECHNOLOGY REPORT FORM

NASA requires that each grantee and grantee subcontractor disclose new technology items and summarize these disclosures annually and in a new technology final report. New technology items can be disclosed on the NASA Form 666A entitled, "New Technology Disclosure Form". The NASA grantee and grantee subcontractor new technology report forms satisfy all new technology annual and final reporting requirements. Use of these forms is optional; however, an alternate format must at a minimum contain the information required by these forms.

Grantee Name and Address: Dr. Stephen Z.D. Cheng
       University of Akron
       Department of Polymer Science
       Akron, OH 44325-3909

Report Submitted by: Dr. S.Z.D.Cheng/Tammy Chalmers
       Tel. No. (216) 972-7538

NASA Grant Title: "The Study of the Thermal Behavior of a New Semicrystallin Polyimide"

NASA Grant Number: NAG3-1288

NASA Grant Monitor: Lorene Albergottie

Grant Expiration Date: 11/30/91   Today's Date: 5/15/92

Definitions:

A **reportable item** is any invention or discovery, <u>whether or not patentable</u>, that was conceived or first actually reduced to practice during the performance of the grant or subcontract. Large business subcontractors must disclose reportable items as they are discovered and submit a cumulative list of these new technology items on an annual basis and at the completion of the grant or subcontract period.

A **subject invention** is any invention or discovery <u>which is or may be patentable</u> that was conceived or first actually reduced to practice during the performance of the grant or subcontract. Grantees and small business subcontractors must, at a minimum, disclose subject inventions as they are discovered and submit a cumulative list of these new technology items on an annual basis and at the completion of the grant or subcontract period.

Grantees and small business subcontractors are only required to disclose and report patentable items (subject inventions). We request, however, that grantees and small business subcontractors disclose and report both patentable and nonpatentable (reportable) items.

PLEASE COMPLETE THE REVERSE SIDE OF THIS FORM AND MAIL TO KAREN GRASSE, NASA LEWIS RESEARCH CENTER, TU OFFICE - M/S 7-3, CLEVELAND, OHIO 44135.

LEGFR.1 - 1990

NEW TECHNOLOGY REPORT

I General Information

1. Type of Report: ( ) Annual   (X) Final

2. Did any nonpatentable items result from the work perfomed under this grant?
   (X) yes ( ) no

3. Did any subject inventions result from the work performed under this grant?
   ( ) yes (X) no

4. Are new technology items being disclosed with this report?
   (X) yes ( ) no

II New Technology Items

Please provide the title(s) of all new and previously disclosed new technology items conceived or first actually reduced to practice under this grant.

Title	Internal Docket Number	Patent Appl. Filed	Patentable Item	Nonpatentable Item
1. Thermal Properties of a New Polyimide	___	( )	( )	(X)
2. _____	___	( )	( )	( )
3. _____	___	( )	( )	( )
4. _____	___	( )	( )	( )

III Subcontractors

Please complete the following section listing all subcontracts issued to date. Include each subcontractor's name, address, contact person and telephone number.

_____none_____

Attn:_____tel. ( )___-____   Attn:_____tel. ( )___-____

Attn:_____tel. ( )___-____   Attn:_____tel. ( )___-____

THERMAL PROPERTIES OF A TOUGH, NEW SEMICRYSTALLINE POLYIMIDE

Tammy M. Chalmers, Anqiu Zhang, Dexing Shen, Shawn Hsun-Shan Lien,
Chung C. Tso, Patricia A. Gabori, Frank W. Harris
and Stephen Z. D. Cheng*

Institute and Department of Polymer Science, The University of Akron,
Akron, Ohio, 44325-3909

ABSTRACT: Thermal properties of a new semicrystalline polyimide synthesized from 3,3',4,4'-benzophenonetetracarboxylic dianhydride (BTDA) and 2,2-dimethyl-1,3-(4-aminophenoxy)propane (DMDA) have been studied. Heat capacities in the solid and liquid states of BTDA-DMDA have been measured. The heat capacity increase at the glass transition temperature (T_g=230°C) is 145 J/(°C mol) for amorphous BTDA-DMDA. The equilibrium heat of fusion of the BTDA-DMDA crystals has been obtained using wide angle X-ray diffraction and differential scanning calorimetry measurements, and it is 75.8 kJ/mol. Based on the information of crystallinity and the heat capacity increase at T_g, a rigid amorphous fraction is identified in semicrystalline BTDA-DMDA samples. The rigid amorphous fraction represents an interfacial region between the crystalline and amorphous states. In particular, this fraction increases with the crystallinity of the sample which should be associated with crystal sizes, and therefore, with crystal morphology. It has also been found that this polymer has a high temperature crystal phase upon annealing above its original melting temperature. The thermal degradation activation energies of BTDA-DMDA are determined to be 154 kJ/mol and 150 kJ/mol in nitrogen and air, respectively.

* To whom the correspondence should be addressed.

INTRODUCTION

A new semicrystalline polyimide has been synthesized from 3,3',4,4'-benzophenonetetracarboxylic dianhydride (BTDA) and 2,2-dimethyl-1,3-(4-aminophenoxy)propane (DMDA). It has been found that this polyimide (BTDA-DMDA) exhibits a high fracture energy of 4.28 kJ/m^2 measured by the double torsion method, coupled with good tensile, flexural and shear properties [1]. In the first paper of this series [2] we reported the synthesis of monomers and polymers. Also, the crystalline unit cell was determined to be monoclinic with a=0.960 nm, b=0.582 nm, c=2.46 nm and γ=81.1°. This polymer shows a high glass transition temperature (T_g) of 230°C, and a melting temperature (T_m) of 325 °C. This leads to a high usage temperature, and relatively low processing temperature when compared with other thermoplastic semicrystalline polymers. A narrow crystallization window between T_g and T_m of about 100°C has limited the sensitivity of overall crystallization kinetics with temperature, as documented by the observations of crystallization kinetics and crystal morphology. A constant Avrami exponent of 2.3 in the temperature range of 260°C-300°C indicates a fixed dimensionality of crystal growth. Randomly stacked lamellae only act as precursors to spherulites. However, no mature spherulitic texture was found over a range of a few nanometers to micrometers [2]. This morphological feature may serve as one of the reasons for such high toughness of this material.

In this paper, we focus on the thermal properties of the polymer. These include heat capacities in the solid and liquid states, equilibrium thermodynamic transition behavior, interfacial structure between crystalline and amorphous states, and a thermal degradation study.

The importance of knowing the heat capacities of the solid and liquid states in polymers has been long recognized [3-5]. From this data the thermodynamic properties, such as enthalpy, entropy and Gibbs free energy can be derived. This information also provides a precise baseline for the quantitative study of the phase transition behavior. Proper extrapolations of the phase transition data lead to the establishment of equilibrium transition

properties (equilibrium heat of fusion, entropy of fusion, and melting temperature). These data are essential for the further solid state characterization of the polymer, in particular, for determination of crystallinity (w^c) of the polymer when exposed to different thermal treatments. With the heat capacities in the solid and liquid states, one would predict for a semicrystalline polymer that based on the two phase (crystallinity) model

$$w^c = 1 - \Delta C_p(m)/\Delta C_p(a) \tag{1}$$

where $\Delta C_p(m)$ and $\Delta C_p(a)$ are the heat capacity increases at T_g for the semicrystalline and the totally amorphous polymer, respectively. If there is a fraction in the polymer which contributes neither to the glass transition at T_g nor to the heat of fusion at T_m, a "rigid amorphous fraction" exists. This was first found in polyoxymethylene [6] and observed in many thermoplastic polymers [4,5]. As a result, the two phase model cannot be used to describe that system, and

$$w^c < 1 - \Delta C_p(m)/\Delta C_p(a) = f_r \tag{2}$$

where f_r is called a rigid fraction above the glass transition temperature, and the rigid amorphous fraction can thus be calculated as $(f_r - w^c)$.

It has also been observed that annealing BTDA-DMDA at high temperature and long time leads to a second crystalline phase with a higher melting temperature (around 360°C). This phase can be identified through wide angle X-ray diffraction (WAXD) experiments, but no change has been found in crystal morphology.

Finally, thermal degradation of the polymer, which is also important from the viewpoint of processing, is also reported.

EXPERIMENTAL

Materials and Samples. BTDA-DMDA was polymerized in our laboratory

and its detailed synthetic procedure was reported in the first part of this series [2]. The poly(amic acids) were obtained as the first step of polymer synthesis, with an inherent viscosity of 1.6 dL/g in a concentration of 0.5 g/dL at 30°C. The poly(amic acids) were chemically imidized with acetic anhydride and pyridine. The chemical structure of the repeat unit is
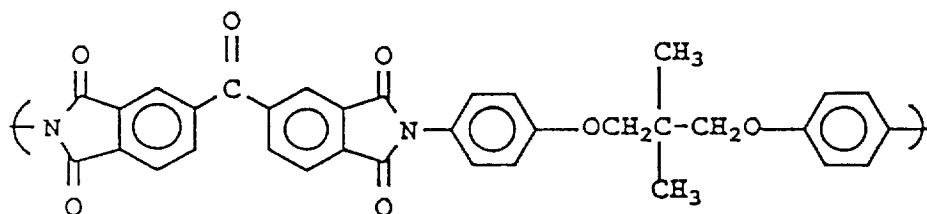
with a molecular weight of 572 g/mol of repeat unit.

Samples prepared for differential scanning calorimetry (DSC) experiments were from both precipitated imidized and compression-molded BTDA-DMDA. The former was heated to 250°C for two hours to ensure complete imidization before introducing any thermal treatment. The later was kept in a compression mold for 20 minutes at 330°C, followed by an annealing step of 30 minutes at different temperatures (260°C-300°C). A typical sample weight of 15 mg was used in both cases. The weights of sample and reference pans were controlled within a deviation of ±0.002 mg. For wide angle X-ray diffraction (WAXD) measurements, the precipitated BTDA-DMDA powders were high-pressure pressed at 290°C to form a thin film with a thickness of 0.5 mm. The films were then thermally treated at different annealing temperatures (260°C-300°C) for 30 minutes before measurements. When the samples were compression molded, the BTDA-DMDA powders were heated to 330°C and held there for 20 minutes under a high pressure. In order to identify the high temperature crystalline phase, a further annealing process to the molded samples at temperatures between 280°C and 320°C for different times was used.

Equipment and Experiments. DSC experiments were carried out via a Perkin-Elmer DSC2 coupled with an IBM computer. The thermal analysis software was provided by MC2. The temperature and heat flow scales were calibrated via standard melting materials of benzoic acid, indium, tin, lead,

zinc, and silver sulfate over a temperature range of 25°C-400°C. The heat capacities were calculated based on the standard Cp of Al_2O_3 (sapphire). Heat capacities of the BTDA-DMDA samples after different thermal treatments were measured under dry nitrogen at 10°C/min. Isothermal crystallization and annealing were performed in the DSC. The samples were heated to 375°C at 10°C/min., and held there for one minute. They were then quenched to preset crystallization temperatures as quickly as experimentally possible. After the samples were held at the temperatures for 30 minutes, they were cooled to 25°C at 10°C/min. Heat capacity measurements for these samples were conducted.

The heat capacity increases at glass transition temperatures for amorphous and semicrystalline samples were determined via heat capacity data following the method previous described [3-5]. On the other hand, the crystallinity was calculated as

$$w^c = \Delta h_f(m) / \Delta h_f^{\circ} \qquad (3)$$

where $\Delta h_f(m)$ and Δh_f° are the heats of fusion of the measured semicrystalline sample and that extrapolated to 100% crystallinity, respectively. Using this information, the existence of a rigid amorphous fraction was determined using equation (2).

The glass transition temperature is usually characterized as a temperature region. Five temperatures are needed to represent the glass transition region. The first perceptible beginning of the glass transition, T_b, is judged by the first increase in heat capacity from that of the solid state (glassy or crystalline). The extrapolated beginning and end of the glass transitions T_1 and T_2 are indicative of the broadness of the major portion of the glass transition. The glass transition temperature T_g is chosen at half-devitrification observed by heat capacity increase.

In order to determine the equilibrium heat of fusion, WAXD experiments were carried out on a Rigaku 12 kW rotating anode with a diffractometer. The scanning angle range was from 5° to 50°. A graphite

crystal was used to ensure that the X-ray incident beam was monochromatic at Cu K_α with a wavelength λ of 0.154 nm. The BTDA-DMDA samples with different thermal treatments were measured. Their crystallinities were calculated following Ruland's method [7] by subtracting the amorphous halo obtained from a quenched sample.

Apparent crystal sizes in the BTDA-DMDA crystals were calculated using widths at half-height of WAXD peaks and the Scherrer equation [8]:

$$L(hkl)=K\lambda/[(B^2-b^2)^{1/2}]\cos\theta \qquad\qquad (4)$$

where B and b are the width at half-height of the diffraction peaks of (hkl) planes and the broadening factor, respectively, and K is a geometry-dependent constant, which is here equal to unity.

Thermo-oxidative and thermal stability were determined using a TA 2950 thermogravimetric (TG) analyzer. The temperature scale was calibrated over the range of interest using a five point temperature method. Thermal degradation activation energies in air and nitrogen atmospheres were obtained using isothermal experiments. Nonisothermal experiments provide the percentage of weight loss at each temperature for a certain heating rate. A typical sample weight of about 10 mg was used for the study.

RESULTS AND DISCUSSION

Heat Capacities of the Solid and Liquid States. DSC measurements provide heat capacities (C_p) of the solid and liquid states for BTDA-DMDA. Figure 1 shows one example of the heat capacity data over ten DSC runs. Below T_g=230°C the heat capacity in the solid state is observed, while above T_m=325°C, that in the liquid state is seen. Between 230°C and 325°C is a transition region where the crystallization and crystal melting are obvious. After curve-fitting of the heat capacity data, the solid state C_p in between -50°C and 200°C shows a linear relationship with temperature:

$$C_p = 1.8901T + 57.4 \qquad\qquad \text{in } J/[(273 + °C) \text{ mol}] \qquad (5)$$

with a root mean square (rms) deviation of ±1.2% obtained by averaging fourteen DSC runs. On the other hand, the liquid state C_p measured above the crystal melting can be expressed as

$$C_p = 0.8159T + 742.7 \qquad\qquad \text{in } J/[(273 + °C) \text{ mol}] \qquad (6)$$

with a rms deviation of ±1.5% obtained by averaging eleven DSC runs.

The heat capacities of the solid and liquid states provide not only the essential information needed to calculate other thermodynamic functions, such as enthalpy, entropy and Gibbs free energy, but also a precise baseline for the study of transition behavior [3-5]. For amorphous BTDA-DMDA at $T_g = 230°C$, one can calculate the heat capacity increase at T_g for BTDA-DMDA based on both heat capacities in the solid and liquid states, and it is 145 J/(°C mol). If one considers that the heat capacity increase at the glass transition temperature for each mobile unit is 11.3 J/(°C mol) [9], the total number of mobile units in this polyimide is close to 14. This yields a heat capacity increase of 165 J/(°C mol), which is about 20 J/(°C mol) higher than the experimental data. The reason for this deviation may be two fold. The division of a repeating unit into mobile units is not wholly unambiguous. One expects independent motion between the different rotational isomers for a mobile unit, for example, methylene groups, carboxyl groups and phenylene groups, etc. Moreover, the effect of a mobile unit is size-dependent. It has been found that "large units", such as phenylene groups and naphthlene groups, seem to contribute twice or even thrice to the heat capacity increase [3-5,10]. Second, the diamine in BTDA-DMDA is similar in structure to polycarbonate in that it contains a bisphenyl A type of structure. The experimentally observed heat capacity increase at T_g for polycarbonate is also smaller than that predicted by the 11.3 J/(°C mol) rule [11]. This indicates that the deviation of the heat capacity increase in BTDA-DMDA from the predicted value is perhaps attributed to the diamine component. Nevertheless, the mechanism of such deviation is not known at this

moment. This may be associated with the cooperative mobility of the 2,2-dimethyl unit in the diamine.

Glass Transitions in Semicrystalline Samples. Table 1 lists the glass transition temperatures and heat capacity increases of BTDA-DMDA samples crystallized under different isothermal conditions. It is clear that the glass transition temperatures of the semicrystalline samples are about 5°C higher than that of the quenched samples as shown in Figure 1. Furthermore, the glass transition regions, which are characterized by ΔT_1 and ΔT_2, are also broadened. This indicates that the existence of the crystalline phase hampers the mobility of the chain molecules and broadens the molecular relaxation process. Similar observations have also been reported for other thermoplastic polymers, such as poly(aryl ether ether ketone) (PEEK), poly(phenlene sufide) (PPS), other polyimides etc. [12-17]. However, different from other polymers which show a decrease in T_g with increasing isothermal crystallization temperature (T_c), the T_g of BTDA-DMDA is almost invariant after the crystallization is completed in the crystallization temperature range between 260°C and 300°C. It is generally understood that with increasing T_c the crystal morphology in the polymers gradually changes (see below). A constant T_g of semicrystalline BTDA-DMDA samples at different crystallization temperatures may be an indication that the morphological change with temperature in BTDA-DMDA is not too severe (see below). This has been illustrated by a narrow crystallization window and lack of spherulitic texture as we reported in the first part of this series [2]. This feature should be very important in the application of fiber-reinforced composites.

By knowing the heat capacity increases of 100% amorphous and semicrystalline samples, one can easily calculate the mobile amorphous portion in the samples after the glass transition via the ratio of $\Delta C_p(m)/\Delta C_p(a)$. The rigid fractions in the samples above the glass transitions are thus obtained through equation (2), and listed in Table 2.

Crystallinity and Apparent Crystal Size. Figure 2 shows a set of WAXD patterns for BTDA-DMDA crystallized at different temperatures and times. It is clear that the intensities of diffraction increase with crystallization temperatures and times. When one uses Ruland's method to determine the crystallinity and DSC to measure the heat of fusion of the samples, Figure 3 illustrates the relationship between these two quantities. Extrapolation to 100% crystallinity in this relationship yields a heat of fusion of 75.8 kJ/mol, recognized as the equilibrium heat of fusion of BTDA-DMDA. A careful observation of Figure 2 indicates that the width at half-height of the WAXD patterns for each diffraction peak is not significantly changed with different crystallization temperatures and times although the crystallinity varies over a range of 10%. Since the width at half-height of the WAXD diffraction peaks is inversely proportional to the apparent crystal size along the crystallographic planes [equation (4)], Figure 4 shows that along the different crystallographic planes, for example, the apparent crystal sizes are around 7-11 nm in the whole crystallization temperature and time ranges studied. One can thus conclude that the crystals in BTDA-DMDA do not perfect with increasing temperature and time. The crystals can only be developed to a certain stability and perhaps size. This may be associated with a mismatch of the molecular packing during the polymer crystallization. Another possible reason is the narrow crystallization window between T_g and T_m. Furthermore, a high primary nucleation density, observed from polarized light microscopy [2], may lead to a limitation in crystal size caused by impingements [18]. It has also been reported that from transmission electron microscopy only randomly stacked lamellar crystals exist. No mature spherulitic texture was seen [2].

Upon annealing, a second high temperature crystal phase can be identified (see below). However, no significant changes on the crystallinity and apparent crystal size are observed.

Crystal Melting and Rigid Amorphous Fraction. From DSC experiments, as shown in Figure 5, the heating traces of the isothermally crystallized samples generally show two melting peaks: a low melting peak which is about 20°C above the isothermal crystallization temperature, and a

high melting peak at around 325°C. The low melting peak usually is small, less than 5% of the total of heat fusion. This portion of the heat of fusion slightly increases with crystallization temperature. In contrast to other thermoplastic polymers such as PEEK, PPS and polyesters [10-17], the two melting peak phenomenon is not predominant in this case. As it has been actively discussed recently [10,17,19-22], this phenomenon may be attributed to two reasons. The low melting crystals may be developed first, and the high melting peak is the result of perfection of these low melting crystals during annealing. On the other hand, two different crystalline morphologies may exist during crystallization. The high melting peak is due to the melting of the dominant lamellar crystals, which were formed first; and the low melting peak is due to the melting of in-filling lamellar crystals located between them, which were formed latter [21]. Since BTDA-DMDA only shows more or less a single morphology, randomly stacked lamellar type [2], one should expect that the two melting peak phenomenon must not be a dominant process. This expectation fits well with our experimental observations. A small low melting peak may be an indication that a very small amount of secondary crystallization occurred after the randomly stacked lamellar crystals were formed.

Different heats of fusion are also observed for the samples crystallized at different temperatures and times. The value can reach as high as 35-40 kJ/mol after the samples had undergone solvent-induced crystallization. In general cases, compression molded samples show the heat of fusion ranging from 10 to 25 kJ/mol. The weight fraction crystallinity was determined by using both DSC and WAXD methods. The data are listed in Table 2, coupled with the rigid fraction (f_r) calculated via equation (2) and the rigid amorphous fraction (f_r-w^c). It is interesting that the rigid amorphous fraction increases with crystallinity. This should be understood from a morphological point of view. Based on the facts that no spherulitic texture was observed in BTDA-DMDA, only randomly stacked lamellae are found, and the apparent crystal size is almost independent of crystallization conditions, we speculate that the crystallinity increase should be proportional to the increase of interfacial area between the crystalline and amorphous regions. This certainly leads to an increase in the amount of rigid amorphous fraction

as long as the crystal morphology and interface structure remain invariant. It is in contrast with other thermoplastic materials such as PEEK, PPS et al. [10-17]. In those cases, the rigid amorphous fractions decreased with increasing crystallization temperature. This is because the crystallization process played an important role in these polymers. At low crystallization temperatures, the overall crystallization rate was fast, evidenced by both low nucleation barriers of primary and surface nucleations and immobile chain molecules. As a result, high nucleation density and small crystal size (both lamellar thickness and lateral size) are apparent. Chain molecules in the isotropic melt may not have enough time to undergo a large conformational change to crystallize into the crystal lattice. Instead, they may only require some local adjustments to fit into the crystals. Tie molecules, long loops and cilia may act as connections to the amorphous region. Internal stress concentrations on the boundary between the crystal and amorphous states should thus cause the rigid amorphous fraction. On the other hand, the overall crystallization rate at high crystallization temperatures is slow, with a relatively high chain molecular mobility. Chain molecules thus have more time to rearrange themselves. Crystal sizes are increased, and crystals are more perfect. As a result, the connection between these two states are thus expected to decrease. Consequently, the rigid amorphous fraction is reduced. Nevertheless, this is not the case in BTDA-DMDA. Based on the experimental observations obtained, one may judge that the true crystalline structure must be thought of as somewhere between adjacent reentry folding [18,23] and the switchboard models [24,25].

It is also interesting to observe that an even higher melting peak exists in the molded samples after further isothermal annealing at different temperatures. This higher melting peak temperature is around 360°C, which is about 30°C-40°C higher than the normal melting peak observed during heating of quenched BTDA-DMDA samples (Figure 1). The temperature and heat of fusion of this peak increase with annealing temperature and time, as shown in Figure 6. The formation of this melting peak is due to the new crystalline phase formed during the molding process when the samples were kept at high isothermal temperature (330°C) for a long time (20 minutes). Figure 7 shows two WAXD powder patterns for the

samples with and without annealing after crystallization. It is clear that one new diffraction peak at 2θ=18° has developed during the annealing. The diffraction peak at 2θ=22.4° is substantially broadened and shifted to lower angle. This might be an indication of an overlapping of the two diffraction peaks, one of which is newly developed. Nevertheless, the overall heat of fusion in the samples is almost constant. Namely, the increase in heat of fusion in the high melting peak is accompanied by a decrease of that for the low melting peak with increasing annealing time. The recognition of this high temperature crystalline phase is also important from a practical point of view. Serving as a matrix resin in high-temperature composites, the development of this phase after processing may provide further stability of the engineering properties at high temperatures.

Thermo-oxidative and Thermal Stability. Nonisothermal TG experiments of BTDA-DMDA in its dry powder form and its molded form were carried out. No difference in the decomposition behavior between these two forms was found. Figure 8 clearly shows the occurrence of decomposition as a two-stage process when the nonisothermal TG experiment was carried out under nitrogen atmosphere. The first of these stages occurred from 410°C to 500°C, followed by the second stage from 500°C to 700°C. At the end of the second stage the polymer still has 35% of its weight remaining.

Figures 9 and 10 are the isothermal experimental data for the percentage weight loss in both nitrogen between 300°C and 500°C and air atmospheres between 300°C and 400°C. Based on an integrated rate expression suggested by Flynn [26], one can follow the equation of

$$\ln t = \ln[g(\alpha)] - \ln A + E_a/(RT) \qquad (7)$$

where t is the isothermal time, $g(\alpha)$ is the integration of the rate of weight loss, A is the pre-exponential factor, R is the gas constant, and E_a is the thermal degradation activation energy. The slope of a plot of ln t and 1/T at

constant fractional loss (α) yields the activation energy of 154 kJ/mol in the nitrogen atmosphere and 150 kJ/mol in the air atmosphere. These values are slight lower than that of PPS at 160 kJ/mol [27]. It is surprising that the activation energies in the air and nitrogen atmospheres are so close to each other. This must be associated with detailed degradation mechanisms in both cases, and further experiments (such as TG coupled with infrared and/or mass spectroscopy) have to be carried out before a definitive conclusion can be reached.

CONCLUSION

We have reported here the thermal properties and transition behavior of a new tough semicrystalline polyimide, BTDA-DMDA. The equilibrium heat of fusion of the BTDA-DMDA crystal is 75.8 kJ/mol. For amorphous BTDA-DMDA, its glass transition temperature is 230°C with a heat capacity increase of 145 J/(K mol). Based on these pieces of information, one can examine the validity of the two-phase (crystallinity) model in this polymer. It has been found that a rigid amorphous fraction exists in the semicrystalline samples which does not become mobile above its glass transition and does not contributed to the crystal melting either, but relaxes at higher temperatures between the glass transition and melting temperatures. It is logically expected that this fraction is representative of the interfacial region between crystalline and amorphous states. Quantitative assessment of this fraction is the first step towards a better understanding of the interface structure in semicrystalline polymers. Particularly, BTDA-DMDA has shown an increase of the rigid amorphous fraction with its crystallinity. This new phenomenon may be understood by the morphological observation of a constant crystal size. It has also been found that a second, high-temperature crystalline phase exists, with a melting temperature around 360°C. Finally, the thermal and thermo-oxidative stability has also been studied.

REFERENCES

1. Harris, F. W.; Lien, S. H.-S.; Zhang, Y.-D.; Tso, C. C.; Gabori, P. A.; Cheng, S. Z. D. *Polymer Preprints, ACS Polym. Chem. Div.* **1991**, *32(2)*, 201.

2. Cheng, S. Z. D.; Mittlemen, M. L.; Zhang, A.-Q.; Shen, D.-X.; Chalmers, T.; Lien, S. H.-S.; Tso, C.-C.; Gabori, P. A.; Harris, F. W. *Polym. Internl.* in press.

3. Wunderlich, B.; Cheng, S. Z. D. *Gazzetta Chimica Italiana,* **1986,** *116,* 345.

4. Cheng, S. Z. D. *J. Appl. Polym. Sci. Appl. Polym. Sympo.* **1989,** *43,* 315.

5. Wunderlich, B.; Cheng, S. Z. D.; Loufakis, K. *"Thermodynamic Properties of Macromolecules"*, in Encyclopedia of Polymer Science and Engineering, Second Ed., Vol. 16, pp. 767, John Wiley & Sons: New York, 1989.

6. Susuki, H.; Wunderlich, B. *Br. Polym. J.* **1985,** *17,* 1.

7. Ruland, W.; Dewaelheyns, A. *J. Sci. Instrum.* **1966,** *44,* 236; see also, *Faserforsch. Textiltechnik* **1967,** *18,* 59.

8. Sherrer, P. *Nach. Ges. Wiss. Gottingen* 98, 1918; see also, in *Kolloid-Chem.* Zsigmondy R. Ed.; Leipzig, 1920.

9. Wunderlich, B. *J. Phys. Chem.* **1960,** *64,* 1052.

10. Cheng, S. Z. D.; Pan, R.; Bu, H.-S.; Wunderlich, B. *Die Makromol. Chem.* **1988,** *189,* 1579.

11. Cheng, S. Z. D.; Wunderlich, B. *J. Polym. Sci. Polym. Phys. Ed.* **1986,** *24,* 1755.

12. Cheng, S. Z. D.; Cao, M. Y.; Wunderlich, B. *Macromolecules* **1986,** *19,* 1868.

13. Cheng, S. Z. D.; Wunderlich, B. *Macromolecules* **1987,** *20,* 1630.

14. Cheng, S, Z, D,; Wu, Z.-Q.; Wunderlich, B. *Macromolecules* **1987,** *20,* 2082.

15. Cheng, S. Z. D.; Wunderlich, B. *Macromolecules* **1988,** *21,* 789.

16. Cheng, S, Z, D,; Pan, R.; Wunderlich, B. *Die Makromol. Chem.* **1988,** *189,* 2243.

17. Cheng, S. Z. D.; Heberer, D. P.; Lien, S. H.-S.; Harris, F. W. *J. Polym. Sci. Polym. Phys. Ed.* **1990,** *28,* 655.

18. Wunderlich, B. *Macromolecular Physics,* Vol. 1, Crystal Structure, Morphology, Defects, Academic Press: New York, 1972.

19. Cebe, P.; Hong, S.-D. *Polymer* **1986,** *27,* 1183.

20. Blundell, D. J. *Polymer* **1987,** *28,* 2248.

21. Bassett, D. C.; Olley, R. H.; Al Raheil, T. A. M. *Polymer* **1988,** *29,* 1745.

22. Lee, Y.; Porter, R. S. *Macromolecules* **1987,** *20,* 1336.

23. Geil, P. H. *Polymer Single Crystals,* Wiley-Interscience, New York, 1963.

24. Flory, P. J. *J. Am. Chem. Soc.* **1962,** *84,* 2857.

25. Fischer, E. W.; Schmidt, G. *Agnew Chem.* **1962,** *74,* 551.

26. Flynn, J. H.; Wall, J. *J. Res. Natl. Bur. Stands.* **1966,** *70A,* 487.

27. Day, M. *Polym. Eng. Sci.* **1989,** *29,* 19.

Table 1. Thermal Properties of BTDA-DMDA in the Glass Transition Region Measured at a Heating Rate of 10°C/min

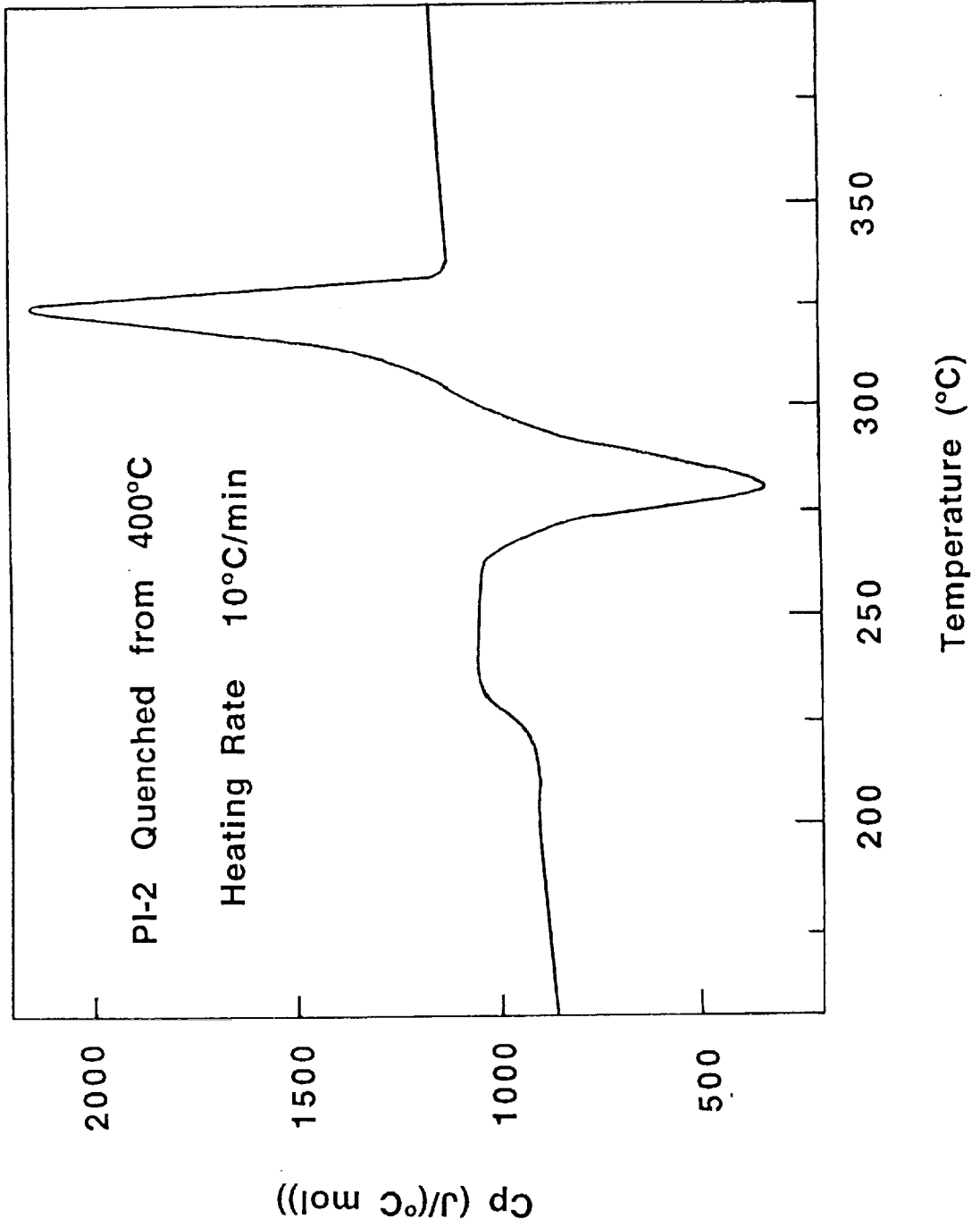| T_c(°C) & t_c(min)	T_b(°C)	T_1(°C)	T_g(°C)	T_2(°C)	T_e(°C)	ΔT_1(°C)*	ΔT_2(°C)*	ΔC_p
quenched	210	220	230	237	240	30	17	145
260, 5	210	221	232	239	250	40	18	75
260, 30	210	225	235	245	260	50	20	38
270, 30	211	225	236	245	262	51	20	35
280, 30	210	226	237	245	261	51	19	40
290, 30	212	227	237	247	261	49	20	38
300, 10	211	225	234	244	258	48	19	49
300, 30	211	226	236	247	261	50	21	36

* $\Delta T_1 = T_e - T_b$, and $\Delta T_2 = T_2 - T_1$

Table 2. Crystallinities and Rigid Amorphous Fractions of BTDA-DMDA Measured at a Heating Rate of 10°C/min

T_c(°C) & t_c(min)	ΔC_p [J/(°C mol)]	f_r (%)	w^c (%)	f_r-w^c (%)
260, 5	75	48	15	33
260, 30	38	74	24	50
270, 30	35	76	25	51
280, 30	40	72	23	49
290, 30	38	74	24	50
300, 10	49	66	20	46
300, 30	36	75	25	50

Figure Legends

Figure 1. A heat capacity measurement via DSC for a BTDA-DMDA sample quenched to liquid nitrogen before heating.

Figure 2. Set of WAXD powder patterns for BTDA-DMDA samples crystallized at different temperatures.

Figure 3. Relationship between the crystallinity measured via WAXD and the heat of fusion measured via DSC for BTDA-DMDA samples.

Figure 4. Apparent crystal sizes along the different crystalline planes at different crystallization temperatures.

Figure 5. DSC heating traces of the BTDA-DMDA samples crystallized at different temperatures after cooling to 25°C at 10°C/min.

Figure 6. DSC heating traces of the BTDA-DMDA molded samples (330°C for 20 minutes) after further annealing at different temperatures and times.

Figure 7. Two WAXD powder patterns of BTDA-DMDA samples with (a) and without (b) annealing.

Figure 8. Nonisothermal TG experiments of powder and molded BTDA-DMDA samples.

Figure 9. Isothermal TG experiments in nitrogen at different temperatures.

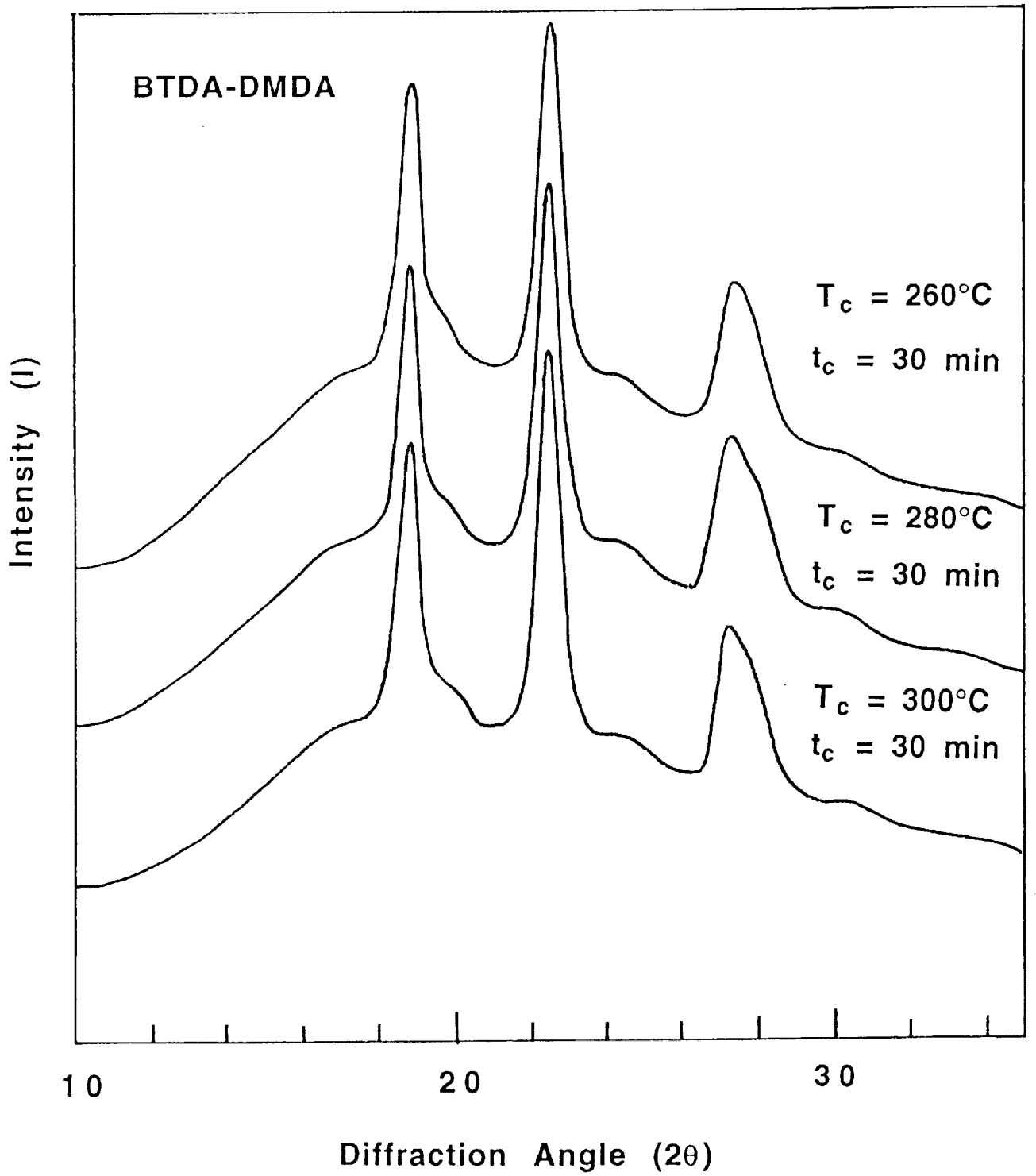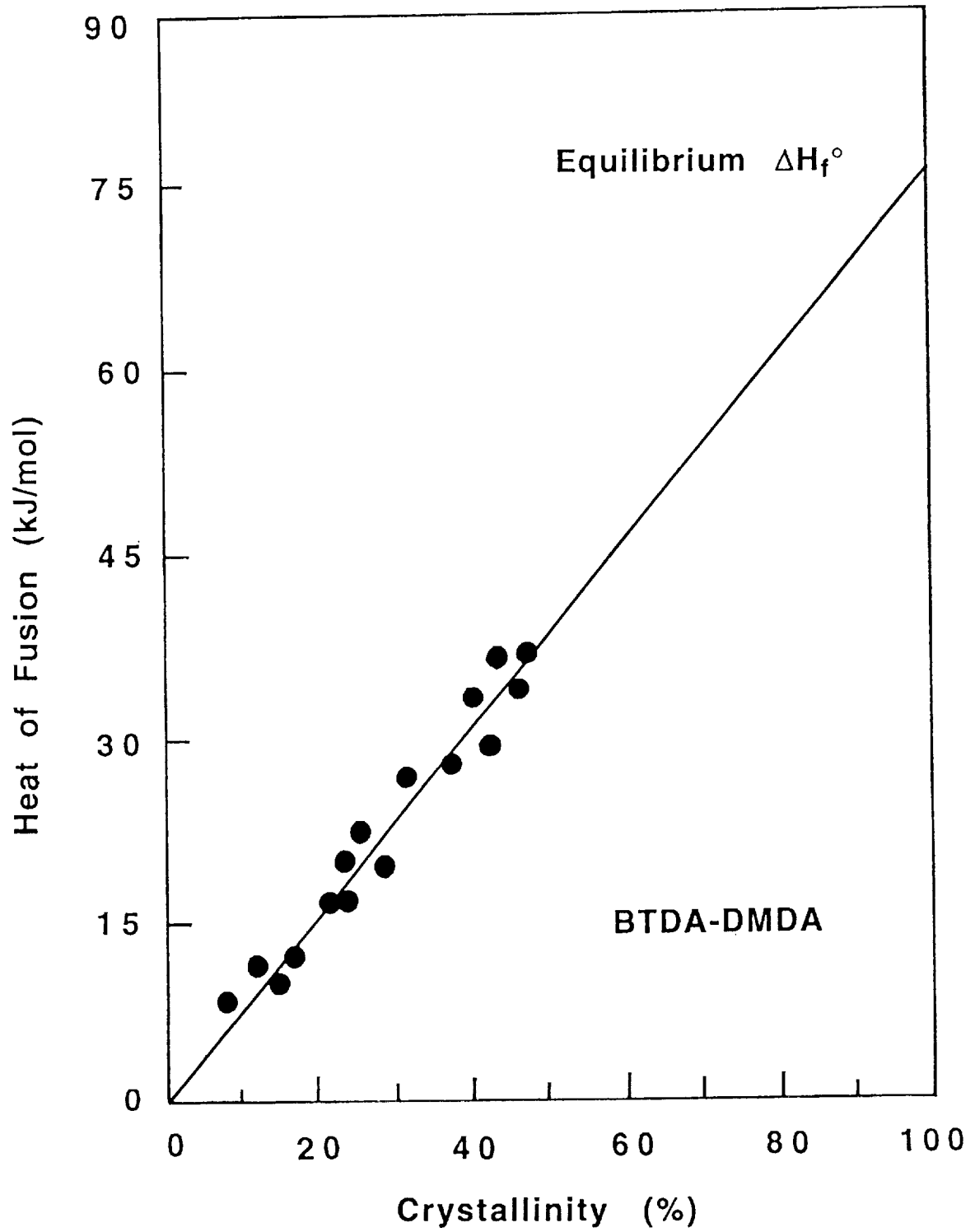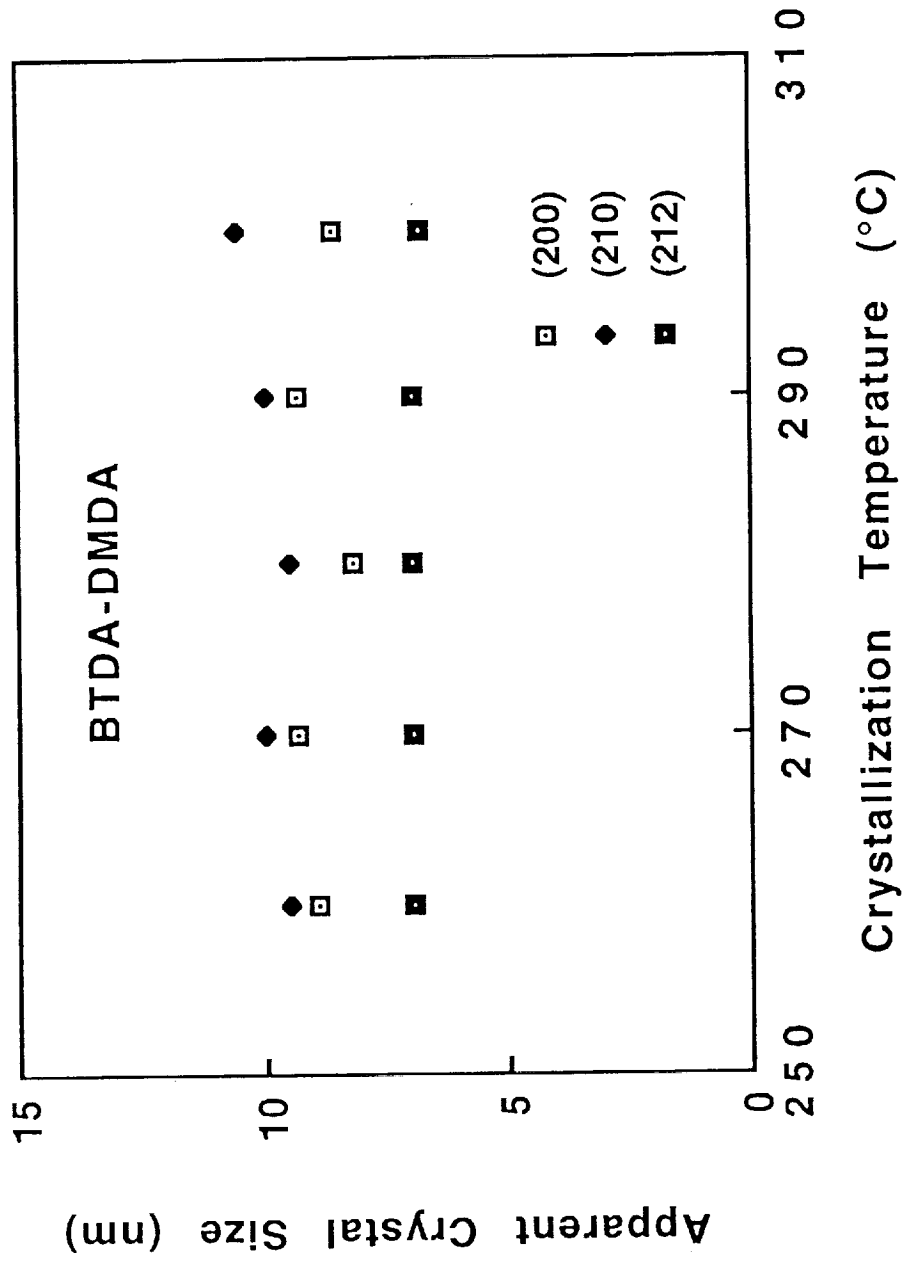Figure 10. Isothermal TG experiments in air at different temperatures.

PI-2 Quenched from 400°C

Heating Rate 10°C/min

Cp (J/(°C mol))

Temperature (°C)

Fig. 2

Fig. 3

BTDA-DMDA

Apparent Crystal Size (nm)

Crystallization Temperature (°C)

☐ (200)
◆ (210)
■ (212)

Fig. 4

BTDA-DMDA

Heating at 10 °C/min
after Isothermal
Crystallization

$\boxed{\quad}$ 500 J/(°C mol)

T_c = 290°C, t_c = 30 min

T_c = 270°C, t_c = 30 min

T_c = 260°C, t_c = 30 min

Heat Capacity [J/(°C mol)]

Temperature (°C)

200   250   300

Fig. 6

Annealing at 300°C for
30 min After the sample
was kept at 330°C
for 20 min

After crystallization
at 280°C for 30 min

BTDA-DMDA

Intensity (I)

Diffraction Angle (2θ)

10　20　30

Thermal Degradation in N2

Heating Rate 10°C/min

PI-2

Temperature (°C)

Weight Loss (%)

Weight (%)

Time (min)

T(°C)

300
320
380

430
440
460
470
480
500

Isothermal

Degradation in Nitrogen

PI-2

Isothermal Degradation in Air

PI-2

T(°C)

300
320
340
380

Time (min)

Weight (%)